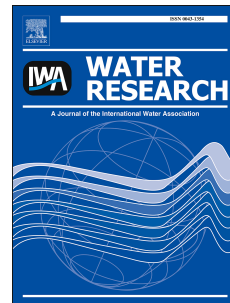


© <2019>. This manuscript version is made available under the CC-BY-NC-ND 4.0 license
<http://creativecommons.org/licenses/by-nc-nd/4.0/>
The definitive publisher version is available online at
<https://doi.org/10.1016/j.watres.2019.03.069>

Accepted Manuscript

Enhancement in adsorption potential of microplastics in sewage sludge for metal pollutants after the wastewater treatment process

Xiaowei Li, Qingqing Mei, Lubei Chen, Hongyuan Zhang, Bin Dong, Xiaohu Dai, Chiquan He, John Zhou



PII: S0043-1354(19)30207-6

DOI: <https://doi.org/10.1016/j.watres.2019.03.069>

Reference: WR 14558

To appear in: *Water Research*

Received Date: 22 October 2018

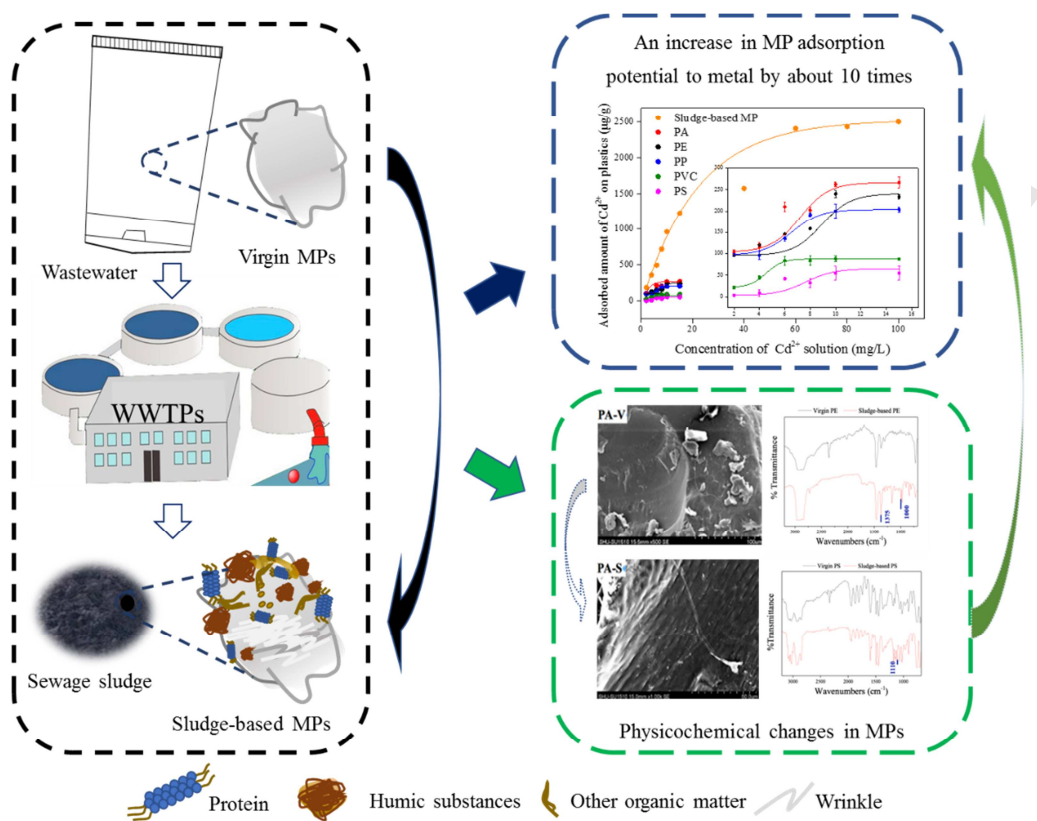
Revised Date: 4 March 2019

Accepted Date: 5 March 2019

Please cite this article as: Li, X., Mei, Q., Chen, L., Zhang, H., Dong, B., Dai, X., He, C., Zhou, J., Enhancement in adsorption potential of microplastics in sewage sludge for metal pollutants after the wastewater treatment process, *Water Research* (2019), doi: <https://doi.org/10.1016/j.watres.2019.03.069>.

This is a PDF file of an unedited manuscript that has been accepted for publication. As a service to our customers we are providing this early version of the manuscript. The manuscript will undergo copyediting, typesetting, and review of the resulting proof before it is published in its final form. Please note that during the production process errors may be discovered which could affect the content, and all legal disclaimers that apply to the journal pertain.

Graphical abstract



ACCEPTED TEL

1 **Enhancement in adsorption potential of microplastics**
2 **in sewage sludge for metal pollutants after the**
3 **wastewater treatment process**

4 Xiaowei Li¹, Qingqing Mei¹, Lubei Chen¹, Hongyuan Zhang¹, Bin Dong^{2*}, Xiaohu
5 Dai^{2*}, Chiquan He¹, John Zhou³

6 ¹School of Environmental and Chemical Engineering, Institute for the Conservation
7 of Cultural Heritage, Shanghai University, Shanghai 200444, People R. China

8 ²State Key Laboratory of Pollution Control and Resources Reuse, National
9 Engineering Research Center for Urban Pollution Control, College of Environmental
10 Science and Engineering, Tongji University, Shanghai 200092, People R. China

11 ³School of Civil and Environmental Engineering, University of Technology Sydney,
12 15 Broadway, Sydney, NSW 2007, Australia

13 *Corresponding Author

14 Phone: 86-021-66137746; Email addresses: lixiaowei419@shu.edu.cn (Dong B.);

15 daixiaohu@tongji.edu.cn (Dai X.)

16 Abstract

17 Microplastics (MPs) as new pollutants of environmental concern have been
18 widely detected in sewage sludge, and may act as significant vectors for metal
19 pollutants due to their adsorption property. Our findings show that Cd, Pb, and Co, but
20 not Ni, contents in sewage sludge are lower than that of corresponding metal ions
21 adsorbed on sludge-based MPs, indicating that the MPs accumulate such metal
22 pollutants as Cd in the sludge samples. In contrast to virgin MPs, sludge-based MPs are
23 one order of magnitude higher adsorption capacity for Cd, which reaches up to 2.523
24 mg g⁻¹, implying that there is a considerable enhancement in adsorption potential of the
25 MPs for metals after the wastewater treatment process. SEM analysis shows that
26 sludge-based MPs have rougher and more porous surface than virgin MPs, and FTIR
27 spectra reveal that functional groups such as C-O and O-H are found on sludge-based
28 MPs. Further, two-dimensional FTIR correlation spectroscopy indicates that C-O and
29 N-H functional groups play a vital role in the process that sludge-based MPs adsorb
30 Cd, which are not found in virgin MPs. The results imply that increased adsorption
31 potentials of the sludge-based MPs to Cd are attributed to changes in the MP
32 physicochemical properties during wastewater treatment process. In addition, such
33 factors as pH value, and sludge inorganic and organic components also have an effect
34 on the MP adsorption to Cd. Principal component analysis shows that the MPs could be
35 divided into three categories, i.e. polyamide, rubbery MPs (polyethylene and
36 polypropylene) and glassy MPs (polyvinyl chloride and polystyrene). Their adsorption
37 potentials to Cd follow the decreasing order: polyamide > rubbery MPs > glassy MPs.

38 In summary, these findings indicate that MPs may exert an important influence on fate
39 and transport of metal pollutants during sewage sludge treatment process, which
40 deserves to be further concerned.

41 **Keywords:** Microplastics; Sewage sludge; Wastewater treatment process; Metal
42 pollutants; Potential risk
43

44 1. Introduction

45 Many researchers have found that wastewater treatment plants (WWTPs) are
46 important sources of microplastics (MPs) (Murphy et al. 2016). The number of MPs
47 decreases gradually during the different treatment stages, such that less than 3% of the
48 MPs are released into effluent (Lares et al. 2018, Talvitie et al. 2017). Thus, most MPs
49 are retained in sewage sludge (Lares et al. 2018, Mahon et al. 2017, Mason et al. 2016,
50 Talvitie et al. 2017). In our previous work, an average of $22.7 \pm 12.1 \times 10^3$ MP particles
51 per kilogram of sewage sludge dry weight were detected (Li et al. 2018c). Using the
52 sludge for agricultural applications means placing MPs directly into the soil, and
53 researchers have estimated that 63 000–430 000 and 44 000–300 000 tons of MPs enter
54 into the soil system annually when sewage sludge is applied to land in Europe and
55 North America, respectively (Nizzetto et al. 2016), exceeding the estimated 93 000–
56 236 000 tons of MPs present in surface water (Sebille 2015). In China, approximately
57 1.56×10^{14} particles of sludge-based MPs are discharged into the soil or other natural
58 environments in 2015 (Li et al. 2018c). However, fate and behavior of the MPs in
59 sewage sludge have yet not to be clarified.

60 MPs act as vectors for pollutants due to their large specific surface area, and pose a
61 potential threat to the environment (Koelmans et al. 2016). Field studies have indicated
62 that persistent organic pollutants (POPs) and metal pollutants adhere to the MPs (Chen
63 et al. 2018a, Koukina et al. 2016, Wang et al. 2017). Organic pollutants adsorbed on the
64 MPs include dichlorodiphenyltrichloroethane, and phenylalanine 17 alpha ethinyl
65 estradiol, etc. (Wang et al. 2015, Wang and Wang 2018, Xu and Liu 2018). Not only can

66 MPs adsorb organic pollutants, but they can adsorb metal pollutants as well. Adsorption
67 of copper (Cu) and zinc (Zn) by polyethylene (PE) and polyvinyl chloride (PVC) has
68 been investigated (Brennecke et al. 2016). Researchers found that MPs derived from
69 sediment have greater adsorption capacities for metal ions than do virgin plastics, likely
70 because the functional groups generated on plastics during the weathering process
71 effectively adsorb metal ions (Holmes et al. 2014).

72 In contrast to unmanaged natural environments (Song et al. 2017, Ter Halle et al.
73 2016), managed man-made environments such as anaerobic digestion and composting
74 can lead to higher biodegradation of plastics such as polylactic acid and
75 polycaprolactone (Narancic et al. 2018). Thus, intensive mechanical abrasion and
76 microbial function during the treatment processes in WWTPs might cause an enhanced
77 effect on physicochemical properties of the MPs, compared to marine and freshwater
78 environment. Mahon et al. (2017) showed that physicochemical properties of MPs in
79 sewage sludge are changed during the treatment processes, for example, the MPs are
80 sheared into smaller sizes in lime stabilization, thermal drying causes their surface to
81 melt and blister, and the MP abundance decreases in anaerobic digestion. However, it
82 is unclear whether these changes affect their potentials to adsorb pollutants.

83 One of the challenges of applying sludge to land is the presence of some metal
84 pollutants such as Pb, Cd, Ni, etc. Owing to their long-term accumulation in soil,
85 humans are exposed to these metal pollutants through food chain (Ken E. Giller 1998,
86 Smith 2009). Hence, we hypothesize that significant changes on physicochemical

87 properties of MPs during the treatment processes may enhance their adsorption
88 potential for metal pollutants. The formation of MP-contaminant combination is
89 potentially harmful to organisms, because the pollutants adsorbed on MPs would
90 desorb in different organ sites (Bakir et al. 2014, Khan et al. 2017, Khan et al. 2015,
91 Kim et al. 2017) and may have additional negative effects on the organism, such as,
92 changes in biological activity of enzyme (Hodson et al. 2017, Kim et al. 2017, Luis et al.
93 2015). Koelmans et al. (2016) suggested that MP ingestion is unlikely to increase the
94 exposure to and thus risks of hydrophobic organic chemicals in marine environment,
95 but Hodson et al. (2017) reported that the existence of MPs could increase the metal
96 exposure in earthworms and enhance the pollutants bioavailability, indicating that
97 MPs can act as vectors of pollutants and increase their risks in the terrestrial
98 environment.

99 Fourier transform infrared (FTIR) spectroscopy is a sensitive tool for exploring
100 chemical structure of MPs, and has been widely applied to characterize them
101 (Cabernard et al. 2018, Hendrickson 2018, Wang et al. 2017). However, it is difficult
102 to detect significant changes in MP spectra during adsorption process of MPs to
103 pollutants using conventional one-dimensional method. Two-dimensional FTIR
104 correlation spectroscopy (2D FTIR COS), as a potential method, can be used to
105 resolve the overlapped peak problems of conventional FTIR spectroscopy, and
106 elucidate the interaction mechanism between MPs and pollutants. By distributing
107 spectral intensity trends within a data set collected as a function of the perturbation

108 sequence (e.g. adsorption time) over a second dimension, one can get
109 cross-correlations that define structural relations (Li et al. 2014). The relative
110 direction and sequencing/ordering of band intensity changes can be determined by
111 synchronous and asynchronous spectra generated with 2D FTIR COS (Chen et al.
112 2018b, Li et al. 2014). The auto-peaks in the synchronous spectrum denote overall
113 susceptibility of the corresponding spectral region to change in spectral intensity as an
114 external perturbation is used to the system. The cross-peaks in asynchronous spectrum
115 probe the specific sequencing/ordering of spectral intensity changes through
116 asynchronous analysis (Noda 2005). In this study, 2D FTIR COS is used to determine
117 order and degree of these changes in main functional groups on the MP surfaces
118 during the adsorption to metal pollutants.

119 The objectives of this study are to: 1) investigate the contents of metals in sewage
120 sludge and those adsorbed on the sludge-based MPs; and 2) compare the adsorption and
121 physicochemical characteristics of virgin and sludge-based MPs for Cd using various
122 techniques, such as adsorption isotherms, X-ray photoelectron spectroscopy, scanning
123 electron microscopy (SEM), microscope FTIR spectroscopy, and two-dimensional
124 FTIR correlation spectroscopy; and 3) explore the effect of such factors as pH value,
125 sludge inorganic matter (silica sand, SS) and organic matter (protein and humic
126 substances) on adsorption potentials of MPs to Cd.

127 **2. Materials and methods**

128 **2.1 Materials and reagents**

129 Three sewage sludge samples were collected from three WWTPs, respectively.
130 The S1 and S2 sludge samples were obtained from the W1 and W2 WWTPs,
131 respectively, in Shenzhen in December 2016, while the S3 sample was collected from
132 the W3 WWTP in Shanghai in September 2017. Physicochemical properties of the
133 sludge samples including pH value, total solids (TS) content, volatile solids (VS)/TS,
134 elemental composition (C, H, N and S), and metal contents were analyzed. Detailed
135 methods for the parameters are provided in the Supporting Information (SI), and the
136 results are shown in Table 1. Table S1 of the SI shows the detailed characteristics of the
137 WWTPs.

138 Virgin MPs including polyamide (PA), polyethylene (PE), polypropylene (PP),
139 polyvinyl chloride (PVC), and polystyrene (PS) were purchased from the Micro
140 Powders Inc., Shanghai, China. Cadmium chloride ($\text{CdCl}_2 \cdot 2.5\text{H}_2\text{O}$), lead nitrate
141 [$\text{Pb}(\text{NO}_3)_2$], nickel nitrate hexahydrate [$\text{Ni}(\text{NO}_3)_2 \cdot 6\text{H}_2\text{O}$], cobalt nitrate hexahydrate
142 [$\text{Co}(\text{NO}_3)_2 \cdot 6\text{H}_2\text{O}$], zinc chloride (ZnCl_2) and copper sulfate pentahydrate
143 ($\text{CuSO}_4 \cdot 5\text{H}_2\text{O}$) all are 99.0% pure and obtained from the Sinopharm Group Corp.
144 Shanghai, China. Metal stock solutions of 1000 mg L^{-1} were prepared using deionized
145 water. All metal standard solutions, standard bovine serum albumin, and commercial
146 humic substances were purchased from the Aladdin Industrial Corp., Shanghai, China.

147 **2.2 MP extraction**

148 The methods used to extract MPs in sewage sludge have been reported in our
149 previous work (Li et al. 2018c). In brief, 100 g of sludge was added to an Erlenmeyer

150 flask with 1000 mL saturated sodium chloride ($1.2 \text{ g mL}^{-1} \text{ NaCl}$). After stirring for 30
151 min, the mixture was allowed to settle for 5 h. Then, the top water was filtered via a
152 vacuum filtration unit using a 37- μm sieve. The extraction was carried out in triplicate,
153 and all the MP extracts were collected in the sieve. The sieve in the vacuum filtration
154 unit was then washed with more than 600 ml distilled water to remove any salt
155 residues. The MP particles were hand-sorted from the filters with fine-tip tweezers
156 under the stereomicroscope, and then carefully rinsed with deionized water to
157 eliminate the attached organic matter (Leslie et al., 2017). After air-drying, the rinsed
158 particles were used for the following adsorption experiment and analysis.

159 **2.3 Batch adsorption experiment**

160 In this experiment, five virgin MPs, i.e., PA, PE, PP, PVC and PS were used to
161 evaluate adsorption property of MPs for metal pollutants, such as Pb, Cd, Zn, Cu, Co
162 and Ni. All metal solutions were prepared by diluting stock solutions with deionized
163 water and adjusting the pH with 0.1 M HCl and 0.1 M NaOH. The adsorption was
164 conducted in centrifuge tubes, each of which contained 0.1 g MP particles and 10 mL
165 aqua of 10 mg L^{-1} metal solution. The tubes were placed on an end-over-end shaker at
166 30 rpm at room temperature for 24 h. Preliminary test showed that 24 h was sufficient
167 to reach adsorption equilibrium (SI Figure S1). The control group was carried out in
168 the same metal solution using the same procedure but without MP particles. Each test
169 including the control, was run in triplicate.

170 Cd was used to compare adsorption capacities of the virgin and sludge-based

171 MPs and investigate the influence of pH value, and sludge components on adsorption
172 capacities of the virgin MPs. Cd solution concentrations used for the virgin MPs were
173 2, 4, 6, 8, 10 and 15 mg L⁻¹, while 2, 4, 6, 8, 10, 15, 20, 40, 60, 80 and 100 mg L⁻¹
174 metal were used for the sludge-based MPs. The pH values ranged from 5.0 to 9.0.
175 Sludge components included inorganic matter (IOM) and organic matter (OM). 0.1 g
176 SS was added to 10 mL aqua of 10 mg L⁻¹ Cd solution with 0.1 g MP, to study the
177 IOM influence on MP adsorption. To analyze the OM influence, protein solutions
178 ranging from 0 to 40 mg L⁻¹ were prepared, while humic substance solutions were
179 used with the contents from 0 to 80 mg L⁻¹. After 24 h of sorption, the MP particles
180 were extracted, and the solutions were filtered using 0.45 µm membrane filter. The
181 metal concentrations in the filtrates were measured using inductively coupled plasma
182 optical emission spectrometer (ICP-OES) as described in the SI, and the metal
183 contents adsorbed on the MPs were calculated by determining the difference between
184 the control and sample filtrate. The MP particles from the tubes were air-dried for the
185 following analysis.

186 **2.4 MP analysis**

187 Chemical composition of the sludge-based MP particles were identified by
188 Microscope Fourier Transform infrared spectrometer (FTIR, IR/NicoletN10 MX,
189 Thermo Fisher Scientific Inc., USA) according to our previous study (Li et al. 2018c).
190 Thermo Scientific Hummel Polymer and Additives FTIR Library and Synthetic Fibers
191 by Microscope FTIR Library were used to analyze the spectra, and then the MP types

192 were determined and percentage of MP in potential MP particles for each WWTP was
193 estimated. The contents of such metals as Cd, Pb, Ni and Co adsorbed on the
194 sludge-based MPs were analyzed as the following method shown in the SI. Shortly,
195 the metals were firstly desorbed into 10% aqua regia from the MP surfaces and then
196 measured by the ICP-OES. SEM analyses was conducted in order to determine the
197 surface structures of the virgin and sludge-based MPs using Hitachi SU-1500
198 scanning electron microscopy (SEM, Hitachi High Technologies Corp., Japan)
199 according to the previous studies as reported by Mahon et al. (2017). X-ray
200 photoelectron spectroscopy (XPS) was applied to measure the Cd content on the
201 surface of MP particles before and after the Cd adsorption experiment using X-ray
202 photoelectron spectrometer (ESCALAB 250, Thermo Fisher Scientific Inc., USA) (Li
203 et al. 2017). FTIR spectra of the virgin and sludge-based MPs were gained through a
204 Nico 380 MX FTIR spectrometer using attenuated total reflectance module (Thermo
205 Fisher Scientific Inc., USA). pH values at the point of zero charge (pH_{PZC}) of the
206 virgin MPs were estimated according to the pH drift method (Yang and Chun 2004).
207 Specific surface areas of the virgin and sludge-based MPs were determined by N_2
208 adsorption-desorption at 77 K with an Autosorb-IQ2 surface area analyzer
209 (Quantachrome Corp., USA).

210 **2.5 Two-dimensional FTIR correlation spectroscopy (2D FTIR COS)**

211 FTIR spectra of the MPs were analyzed using 2D COS according to the references
212 (Li et al. 2015, Li et al. 2014), to further reveal subtle structural variations of the virgin

213 and sludge-based MPs after their interaction with different contents of Cd. The FTIR
 214 spectra were normalized by summing the absorbance from 4000–400 cm^{-1} , and
 215 multiplying by 1000. Subsequently, the normalized data set were transformed into a
 216 new spectral matrix using principal component analysis (PCA) in Matlab R2012b (The
 217 Mathworks, USA) to reduce the level of noise (Babamoradi 2013), and then 2D FTIR
 218 COS maps were conducted using 2D Shige software (Kwansei Gakuin University,
 219 Japan) and re-plotted by Origin 9.0 software (OriginLab Corp., USA).

220 2.6 Data analysis

221 Langmuir, Freundlich and Dubbin-Radushkevich models were applied to fit
 222 adsorption isotherms of Cd on the virgin and sludge-based MPs. The three models can
 223 be described by Equations (1), (2), and (3), respectively.

$$\frac{C_e}{q_e} = \frac{1}{k_L q_{\max}} + \frac{C_e}{q_{\max}} \quad (1)$$

$$\ln q_e = \ln k_F + \frac{1}{n} \ln C_e \quad (2)$$

$$q_e = q_{DR} \exp(-B_{DR} \varepsilon_{DR}^2) \quad (3)$$

224 In which C_e (mg L^{-1}) is the Cd concentration remaining in the solution at equilibrium, q_e
 225 ($\mu\text{g g}^{-1}$) is the amount of Cd adsorbed per mass unit of adsorbent at equilibrium, q_{\max}
 226 ($\mu\text{g g}^{-1}$) is the maximum adsorption capacity, k_L (L mg^{-1}) is the Langmuir binding
 227 constant, k_F ($\text{mg}^{1-n} \text{L}^n \text{g}^{-1}$) and n are Freundlich constants related to the adsorption
 228 capacity and the adsorption intensity, q_{DR} ($\mu\text{g g}^{-1}$) and B_{DR} ($\text{mol}^2 \text{J}^{-2}$) are the D-R

229 isotherm constants and ε_{DR} is the Polanyi potential that is equal to $RT \ln(1 + \frac{1}{C_e})$, where

230 R is the gas constant ($8.314 \text{ J mol}^{-1} \text{ K}^{-1}$) and T is the absolute temperature (K).

231 Different types of MPs were categorized using PCA according to their adsorption
232 properties to Cd in presence of such factors as pH, SS, protein, and humic substances.

233 The data were normalized prior to analysis, to obtain standardized values on the
234 ordination scores. PCA was carried out with the SPSS 13.0 software.

235

236 **3. Results and discussion**

237 **3.1 Metal contents adsorbed on the sludge-based MPs**

238 As shown in Figure 1, the contents of Cd, Pb and Co adsorbed on the sludge-based
239 MPs are higher than those of the corresponding metal ions in sewage sludge, but the Ni
240 content is lower. This indicates that the MPs accumulate some metals in the sludge
241 samples, in accordance to the previous results from the sea and river water. Brennecke
242 et al. (2016) found that metal concentrations on plastics are higher than in the
243 surrounding seawater, indicating that the MPs act as vectors for metal pollutants.
244 Analysis of energy dispersive X-ray spectroscopy showed that the metals carried by
245 MPs are not inherent but are instead derived from the environment, implying that the
246 metal accumulation on the MPs in surface sediment from the Beijiang River (Wang et
247 al. 2017).

248 MP particles extracted from the sewage sludge were identified using microscope
249 FTIR, and the results are shown in Figure S2 of the SI. Primarily, PA, PE, polyolefin

250 (olefin), PS, and alkyd resin (AR) are found in the sludge. To investigate the effect of
251 MP type on metal accumulation, PA, PE, PP, PVC, and PS were used to adsorb Pb, Cd,
252 Zn, Cu, Co, and Ni which are often found in the sewage sludge. In general, the metal
253 contents adsorbed on the MPs decrease in the following order: Pb > Cd > Zn > Cu >
254 Co > Ni. The potential capacities of different MPs for metal adsorption present the
255 following descending order: PA > PE > PP > PVC > PS. Kołodyńska et al. (2012) and
256 Rocha et al. (2009) reported similar results based on the biochar with the following
257 order: Pb > Cd > Cu. Other researchers found the order of organic substances
258 adsorbed on different types of plastics to be PA \geq PE \geq PP > PVC > PS (Li et al.
259 2018a, O'Connor et al. 2016, Wang et al. 2018), consistent with the adsorption results
260 of MPs and metals in this study. Thus, the results imply that the MP type has a
261 significant effect on the adsorption of metal pollutants on MP.

262 **3.2 Comparison of adsorption capacity between virgin and sludge-based MPs**

263 Mahon et al. (2017) found that MPs have the characteristics of melting and
264 blistering after thermal treatment, and shredding and flaking after lime stabilization.
265 These changes in MP physicochemical properties during sludge treatments might
266 cause a significant variation in adsorption potentials of the MPs for metal pollutants.
267 Therefore, adsorption and physicochemical features of the virgin and sludge-based
268 MPs are systematically investigated and compared in this study.

269 As show in Figure 1, high contents of Cd are adsorbed on the virgin and
270 sludge-based MPs. Meanwhile, Cd is one of the most toxic metals due to its solubility,

271 mobility, and biological accumulation potential (Nies 1991), and can be transported
272 into cells, where it can disrupt protein structure and function (Belhalfaoui et al. 2009,
273 Xu et al. 2017). Therefore, Cd is used as a representative metal to evaluate the
274 difference in adsorption of the virgin and sludge-based MPs to metals in this study.

275 XPS analysis shows that two additional Cd3d (405 eV and 411 eV) peaks are
276 observed in XPS spectra of the MPs after the adsorption process (SI Figure S3),
277 compared with the virgin MPs, indicating that Cd is indeed adsorbed on the MPs. Cd
278 adsorption isotherms of the virgin and sludge-based MPs are shown in Figure 2. The
279 isotherms of virgin PA, PE, PP and PS, and sludge-based MP fit the Langmuir model
280 well (Table 2 and SI Figure S4), implying that the adsorptions are monolayer
281 adsorption. The isotherm of PVC fits Freundlich model well, revealing that the
282 adsorption belongs to multilayer adsorption. According to the Langmuir model, Cd
283 adsorption capacity of the sludge-based MPs reaches a maximum of 2.523 mg g^{-1} ,
284 which is one order of magnitude higher than that of the virgin MPs (Table 2),
285 corresponding to the previous results from the comparison of virgin and aged MPs
286 from the nature environment (Holmes et al. 2014, Turner and Holmes 2015,
287 Wijesekara et al. 2018). Holmes et al. (2014) reported greater adsorption of metals on
288 beached (aged) plastics than on virgin plastics. In another study, modified microbeads
289 that were incubated for several days in soils, sediments and biosolids are found to
290 adsorb more Cu than untreated microbeads (Wijesekara et al. 2018).

291 SEM analysis reveals that the surfaces of sludge-based MPs exhibit wrinkled and
292 aggregated structures (Figure 3), in contrast to smooth surfaces of the virgin MPs
293 (Mahon et al. 2017, Wijesekara et al. 2018). Specific surface area of the sludge-based
294 MPs is higher than that of the virgin MPs except for PS (SI Table S2), indicating that
295 more potential adsorption sites exist on the sludge-based MPs. FTIR spectra of the
296 sludge-based MP present some characteristic peaks, distinct from the virgin MPs (SI
297 Figure S5). Compared with virgin PE, the corresponding sludge-based MP shows
298 stronger peaks at 1000–1100 cm^{-1} to the C-O stretching of primary and secondary
299 alcohols, and at 1370–1376 cm^{-1} to the C-H and O-H deformation of alcohol and
300 phenolic groups. The result implies the presence of O-containing (C-O and O-H)
301 groups on the sludge-based MPs, which is possibly attributed to oxidative degradation
302 and erosion of the MPs (Ceccarini et al. 2018), and the attachment of organic matter on
303 them (Wijesekara et al. 2018). Turner and Holmes (2015) showed that the attachment
304 of organic matter to MPs during the weathering process affects the adsorption of
305 metal. Hence, these results indicate that the emergence of O-containing functional
306 groups may play an important role in enhancing metal adsorption potential of the
307 sludge-based MPs.

308 To further understand the role of the functional groups during the MP adsorption
309 to Cd, 2D COS was used to analyze the FTIR spectra. Significant spectral variations
310 are found in the ranges of 900–1300 cm^{-1} and 1350–1600 cm^{-1} , which contain the
311 bands corresponding to amides, carboxylic acids, esters, aliphatic group, and

312 carbohydrates (Li et al. 2015, Li et al. 2014). As shown in Figure 4, four major
313 auto-peaks in synchronous map of the sludge-based MPs follow in the decreasing
314 order: $1580 > 1440 \text{ cm}^{-1}$, implying that N-H functional group plays a greater role in
315 adsorbing metals, compared with C-H functional group. Off-diagonal peaks
316 (cross-peaks) in the synchronous map show correlated signals, implying simultaneous
317 or coincidental changes in spectral intensities at two different spectral variables (Li et
318 al. 2015, Li et al. 2014). Two main cross-peaks at $(1460, 1580)$ and $(1520, 1580) \text{ cm}^{-1}$
319 are positively correlated in the sludge-based MPs, suggesting the simultaneous
320 changes. Three cross-peaks at $(1390, 1580)$, $(1440, 1580)$ and $(1540, 1580) \text{ cm}^{-1}$ show
321 that the bands are correlated negatively, implying that the functional-group changes
322 are not simultaneous. In contrast to synchronous maps of the virgin MPs (SI Figure
323 S6-S9), specific C-O group at 1100 cm^{-1} is observed in that of the sludge-based MPs,
324 complementing and confirming the finding of important role of C-O functional group
325 in metal adsorption on the sludge-based MPs based on FTIR analysis. In the
326 asynchronous map, cross-peaks can provide useful information about sequential order
327 of the changes of different organic functional groups. According to Noda's rule (Noda
328 2005), the band changes follow the order: $1050 \rightarrow 1250 \text{ cm}^{-1}$ and $1580 \rightarrow 1440 \text{ cm}^{-1}$.
329 The structural variation sequence in the adsorption process could be proposed as
330 follows: C-O \rightarrow C-H and N-H \rightarrow C-H. The results indicate that the C-O and N-H
331 functional groups are combined preferentially with Cd during the adsorption,
332 compared with C-H group. The results complement and confirm the findings from

333 FTIR spectra that physicochemical changes of the sludge-based MPs such as
334 generation of O-contain groups result in the enhancement of MP adsorption capacity.

335 Fragmentation of MPs weathered by environment factors like wind, sunlight, and
336 mechanical abrasion in natural environments has been reported widely (Song et al.
337 2017, Ter Halle et al. 2016). However, these processes often require long periods of
338 time (Ceccarini et al. 2018). In contrast to the natural environment, WWTPs are
339 artificial ecosystems in which intensive physical, chemical, and biological processes
340 occur in the presence of high contents of organic matter and various active microbes.
341 MP surface may be abraded by shearing effect attributable to mechanical mixing at
342 “grit & grease” removal stage and/or the aeration at activated sludge tank. Elevated
343 pH in lime stabilization can fragment plastics, resulting in larger quantities and
344 smaller size classes of plastics (Mahon et al. 2017, Zubris and Richards 2005).
345 Microorganisms are critical community during biological treatment process in
346 WWTPs. The MPs are colonized by microbe, leading to the formation of biofilm.
347 PE-degrading bacteria have been found in the biofilm (De Tender et al. 2017), and can
348 cause chain scission and oxidation of PE (Restrepo-Flórez et al. 2014). Therefore, the
349 polymer-degrading bacteria in the biofilms can lead to changes in the MP surface
350 during secondary wastewater treatment processes. Researchers suggested a decrease
351 in MP abundance after sludge anaerobic digestion attributable to the biological
352 breakdown of polymers (Shah et al. 2008, Yoshida 2016). Therefore, wastewater
353 treatment processes cause changes in physicochemical properties of MPs, and thus

354 can enhance their capacity to adsorb such pollutants as metals.

355 **3.3 Factors affecting the Cd adsorption by virgin MPs**

356 Sewage sludge has a broad pH range, and it contains high contents of complex
357 inorganic and organic matter, such as protein and humic substances. Enhancing our
358 knowledge about the influences of environmental factors (e.g., pH value) and sludge
359 components (e.g., inorganic and organic matter) is vital to understand adsorption
360 potential of MPs in sewage sludge to metals.

361 3.3.1 Effect of pH value

362 The adsorption of metal ions depends on pH value of solution because it affects
363 both surface charge of the adsorbent and the speciation of metal ions (Melo and Neto
364 2013). Figure 5A shows that the adsorbed Cd contents on the MPs first increase, then
365 decrease in the range of pH 5-9. The adsorption of Cd on MPs increases as the pH due
366 to the enhancement of the anionic surface, indicating the significance of electrostatic
367 interactions (Wang et al. 2015). A decrease in the adsorption at higher pH is attributed
368 to the formation of precipitation competing with Cd iron for active sites of the MPs,
369 which reduces metal retention (Kołodziejńska et al. 2012, Vimala and Das 2009). The
370 highest adsorbed Cd contents are found at pH 7.7, 7.4, 7.1, 6.0 and 6.0 for PA, PE, PP,
371 PVC and PS, respectively (Figure 5A), indicating that pH value has different
372 influence on different types of MPs for Cd adsorption. The pH_{PZC} (the point of zero
373 charge) is the pH at which the surface of the MP has a net zero charge. At $pH > pH_{PZC}$,
374 the MP surface has a net negative charge and cations can be adsorbed. Table S2 of the

375 SI shows that pH_{PZC} values of the five MPs are 5.59-5.85, and less than the pH at
376 which the highest adsorbed Cd contents are found. The result implies that adsorption
377 of Cd on the MPs belongs to chemical adsorption. The negative charge on the MPs
378 are attributed to negatively charged groups that are bonded chemically to the
379 microsphere during polymerization (Dong 2005, Lu et al. 2018). In this study, pH
380 values of the sewage sludge range from 6.88 to 7.38 (Table 1), indicating that
381 adsorption potentials of the sludge-based MPs shows a high level for metals in terms
382 of pH value.

383 3.3.2 Effect of sludge components

384 Sewage sludge are composed of inorganic particles and organic matter (Wei et al.
385 2018). The percentage of sand in sludge inorganic matter reaches up to 78.9% in China
386 (Zhao 2015), and thus SS was selected as a representative of sludge inorganic
387 component (Duan and Dai 2016) in the study. Sludge organic matter including protein
388 and humic substances might affect adsorption of the MPs to metals (Wei et al. 2016).
389 Organic matter can readily adsorb metals, so it has a potential role in metal transport
390 into the environment and metal sorption to bacterial cells (Hu et al. 2007, Joshi and
391 Juwarkar 2009). Many OM functional groups, such as carboxyl, phosphoric, sulfhydryl,
392 phenolic, and hydroxyl groups, all can complex with metals (Sheng et al. 2010).
393 However, there is little information about the influence of sludge IOM and OM
394 components on the adsorption of metal on MPs.

395 Content of Cd adsorbed on the MPs in SS+MP group is lower than that in the
396 corresponding pure MP group except for PS (Figure 5B). These results imply that
397 inorganic matter in sewage sludge affects metal adsorption of the MPs adversely.
398 Figure 5C shows that Cd content adsorbed on the MPs decreases with the protein
399 concentration, except for PS. Research reported that protein has a net positive charge at
400 pH 7.5 (Matsui et al. 2015). Positively charged protein molecules are attracted to
401 negatively charged surface of the MPs, and thus compete with Cd for adsorption sites
402 on the MPs. As shown in Figure 5D, with the concentration of humic substances, the Cd
403 contents adsorbed on PA, PE, and PP decrease, and on PVC and PS increase. It is
404 well-known that humic substances as common natural organic matter are often
405 negatively charged, and can adsorb cations, causing a decrease in available Cd content
406 for sorption of the MPs. Therefore, the adsorption potentials of PA, PE and PP to Cd
407 reduce as the content of humic substances increases. Researchers also reported that
408 concentrations of adsorbed tetracycline on PS, PP, and PE decreased with an increase in
409 humic substance concentrations (Xu and Liu 2018). On the other hand, humic
410 substances can adhere to the MP surfaces, causing an increase in zeta potentials and
411 negative charge on the MPs surfaces (Li et al. 2018b, Lu et al. 2018), and increasing
412 electrostatic interactions between Cd and the MPs. Chen et al. (2018b) found that the
413 interaction between humic substances and MPs results in formation of the co-polymer.
414 The interaction increases negative surface charges on MPs and enhances their stability

415 (Alimi et al. 2018, Lu et al. 2018). Therefore, the adsorbed Cd contents on PVC and PS
416 increase with humic substances concentration.

417 PCA was used to classify the five MPs, i.e. PA, PE, PP, PVC and PS, according
418 to their maximum Cd adsorption amount and changing characteristics of adsorbed Cd
419 content under the influence of pH, and sludge IOM and OM components. As Figure 6
420 shows, the five MPs are divided into three main categories, Category 1 (PA),
421 Category 2 (PE and PP), and Category 3 (PVC and PS). The above results show that
422 adsorption potentials of the three categories of MPs follow the decreasing order:
423 Category 1 > Category 2 > Category 3. The presence of polar amide functional group
424 (-CO-NH-) and hydrogen bonding on the PA surface might cause its high adsorption
425 capacity to Cd (Li et al. 2018a). According to the glass transition temperatures (T_g),
426 the plastics are divided into two categories, rubbery plastics (PE and PP) and glassy
427 plastics (PVC and PS) (Alimi et al. 2018, Teuten et al. 2009). Rubbery plastics have a
428 large amount of free volume between the molecules, while glassy polymers have a
429 dense structure and closed internal nanoscale pores (Teuten et al. 2009). Therefore,
430 the structure of glassy plastics leads to lower pollutant mobility and slower diffusivity
431 rates than those observed in rubbery plastics, resulting in lower adsorption capacity
432 (Pascall et al. 2005). These results complement and confirm that the MP type has a
433 significant effect on the metal adsorption.

434 **3.4 Implications and limitations of this study**

435 Our results show that MPs can act as vectors for metals in sewage sludge and

436 potentially influence on metal fate and transport when sewage sludge is applied to
437 land. Tons of the MPs enter the soil system annually during sludge land application
438 (Li et al. 2018c, Nizzetto et al. 2016). Organisms take up the metal pollutants
439 adsorbed on the MPs, resulting in the partial accumulation of metal pollutants and
440 increasing their potentials risks. Adsorption capacity of the sludge-based MPs for such
441 metal as Cd is one order of magnitude higher than that on virgin MPs, implying a
442 considerable increase in MP adsorption capacity on the metal after the wastewater
443 treatment process, and thus the sludge-based MPs might produce higher effect to the
444 metal transport than the virgin MPs. The results are attributed to changes in
445 physicochemical characteristics of the MPs during wastewater treatment processes.
446 The MPs are oxidized and/or coated by organic matter, causing an increase in
447 potential adsorption sites and the generation of O-containing group on their surfaces,
448 and thus enhancing their adsorption to metal pollutants. In addition, biofilm formation
449 on the MPs also possibly contributes to the changes. Wu et al. (2017) showed that the
450 presence of plastic colonization could influence transport and transformation of the
451 pollutants. In summary, it requires more attention to the potential risks resulted from
452 metal accumulation on the MPs in sewage sludge.

453 Limitations of this study are that the MPs were gained from the sewage sludge
454 samples through hand picking, and limited amounts were available for experiments.
455 Thus, adsorption properties of different types of the sludge-based MPs to metal
456 pollutants is lack of investigation, and physicochemical changes in the MPs during

457 simulated wastewater treatment processes need to further investigate. Such study will
458 allow us to obtain a profound understanding of the mechanism related to enhanced
459 adsorption of the MPs to metal after the wastewater treatment process. In addition, it
460 is significant to further explore the influence of wastewater treatment processes, both
461 individually and collectively, on the MP adsorption to other pollutants such as other
462 metals and organic pollutants.

463

464 **4. Conclusions**

465 MPs can accumulate the metals in sewage sludge, although the adsorption
466 capacity might differ for different metal ions and plastics types. Adsorption potentials
467 of the MPs to such metal as Cd increase by about ten times during entering into sewage
468 sludge after wastewater treatment processes, compared with virgin MPs. They are
469 resulted from physicochemical changes of the sludge-based MPs during the treatment
470 processes, such as the emergence of rough and porous structures, and the presence of
471 C-O and O-H groups on the MP surfaces. It needs further investigation to understand
472 how wastewater treatment processes to affect MP physicochemical properties in
473 controlled experiments. Analyses of factors affecting the MP adsorption indicate that
474 sludge inorganic and organic components have an adverse effect on metal adsorption
475 potentials on the MPs. However, the influence differs for different MP types, e.g. humic
476 substances seem to enhance adsorption of the glassy MPs to Cd. In sum, ecological risk

477 of metal accumulation on the MPs needs to further investigate during sludge land
478 application.

479

480 **Acknowledgements**

481 The work was financially supported by National Key R&D Program of China
482 (2018YFC1903201), National Natural Scientific Foundation of China (51408423,
483 51578397 and 51538008), Program of Shanghai Technology Research Leader Grant
484 (17XD1420500), Key Program for International S&T Cooperation Projects of China
485 (2016YFE0123500), and Cultural & Heritage Protection Key Innovation Team in
486 Shanghai High-level Local University.

487 **Appendix A. Supplementary data**

488 Additional tables and figures as mentioned in the main text. This supporting
489 information is available free of charge via the Internet.

490 **References**

- 491 Alimi, O.S., Farner Budariz, J., Hernandez, L.M. and Tufenkji, N. (2018)
492 Microplastics and Nanoplastics in Aquatic Environments: Aggregation, Deposition,
493 and Enhanced Contaminant Transport. *Environ. Sci. Technol.* 52, 1704-1724.
- 494 Babamoradi, H., van den Berg, F., Rinnan, Å. (2013) Bootstrap based confidence
495 limits in principal component analysis – a case study. *Chemometr. Intell. Lab.* 120,
496 97– 105.
- 497 Bakir, A., Rowland, S.J. and Thompson, R.C. (2014) Enhanced desorption of
498 persistent organic pollutants from microplastics under simulated physiological
499 conditions. *Environ. Pollut.* 185, 16-23.
- 500 Belhalfaoui, B., Aziz, A., Elandaloussi, E. and Ouali, M.S. (2009) Succinate-bonded
501 cellulose: A regenerable and powerful sorbent for cadmium-removal from spiked
502 high-hardness groundwater. *J. Hazard. Mater.* 169(1-3), 831-837.
- 503 Brennecke, D., Duarte, B., Paiva, F., Caçador, I. and Canning-Clode, J. (2016)
504 Microplastics as vector for heavy metal contamination from the marine environment.

- 505 Estuarine, Coastal Shelf. Sci. 178, 189-195.
- 506 Cabernard, L., Roscher, L., Lorenz, C., Gerdts, G. and Primpke, S. (2018)
- 507 Comparison of Raman and Fourier Transform Infrared Spectroscopy for the
- 508 Quantification of Microplastics in the Aquatic Environment. *Environ. Sci. Technol.*
- 509 52(22), 13279-13288.
- 510 Ceccarini, A., Corti, A., Erba, F. and Modugno, F. (2018) The Hidden Microplastics:
- 511 New Insights and Figures from the Thorough Separation and Characterization of
- 512 Microplastics and of Their Degradation Byproducts in Coastal Sediments. *Environ.*
- 513 *Sci. Technol.* 52(10), 5634-5643.
- 514 Chen, Q., Reisser, J., Cunsolo, S., Kwadijk, C., Kotterman, M., Proietti, M., Slat, B.,
- 515 Ferrari, F.F., Schwarz, A., Levivier, A., Yin, D., Hollert, H. and Koelmans, A.A.
- 516 (2018a) Pollutants in Plastics within the North Pacific Subtropical Gyre. *Environ. Sci.*
- 517 *Technol.* 52(2), 446-456.
- 518 Chen, W., Ouyang, Z.Y., Qian, C. and Yu, H.Q. (2018b) Induced structural changes of
- 519 humic acid by exposure of polystyrene microplastics: A spectroscopic insight.
- 520 *Environ. Pollut.* 233, 1-7.
- 521 De Tender, C., Devriese, L.I., Haegeman, A., Maes, S., Vangeyte, J., Cattrijsse, A.,
- 522 Dawyndt, P. and Ruttink, T. (2017) Temporal Dynamics of Bacterial and Fungal
- 523 Colonization on Plastic Debris in the North Sea. *Environ. Sci. Technol.* 51(13),
- 524 7350-7360.
- 525 Dong, Y. (2005) Radical entry in emulsion polymerization: Propagation at latex
- 526 particles/water interfaces. *J. Colloid Interface Sci.* 288(2), 390-395.
- 527 Duan, N. and Dai, X. (2016) Anaerobic digestion of sludge differing in inorganic
- 528 solids content: performance comparison and the effect of inorganic suspended solids
- 529 content on degradation. *Water Sci. Technol.* 74(9), 2152-2161.
- 530 Hendrickson, E. (2018) Microplastic abundance and composition in western Lake
- 531 Superior as determined via microscopy, Pyr-GC:MS, and FTIR. *Environ. Sci. Technol.*
- 532 52(4), 1787-1796.
- 533 Hodson, M.E., Duffus-Hodson, C.A., Clark, A., Prendergast-Miller, M.T. and Thorpe,
- 534 K.L. (2017) Plastic Bag Derived-Microplastics as a Vector for Metal Exposure in
- 535 Terrestrial Invertebrates. *Environ. Sci. Technol.* 51(8), 4714-4721.
- 536 Holmes, L.A., Turner, A. and Thompson, R.C. (2014) Interactions between trace
- 537 metals and plastic production pellets under estuarine conditions. *Mar. Chem.* 167,
- 538 25-32.
- 539 Ken E. Giller, E.W. (1998) Toxicity of heavy metals to microorganisms and microbial
- 540 processes in agricultural soils - a review *Soil Biol. Biochem.* 30(10/11), 1389-1414.
- 541 Khan, F.R., Boyle, D., Chang, E. and Bury, N.R. (2017) Do polyethylene microplastic
- 542 beads alter the intestinal uptake of Ag in rainbow trout (*Oncorhynchus mykiss*)?
- 543 Analysis of the MP vector effect using in vitro gut sacs. *Environ. Pollut.* 231,
- 544 200-206.
- 545 Khan, F.R., Syberg, K., Shashoua, Y. and Bury, N.R. (2015) Influence of polyethylene
- 546 microplastic beads on the uptake and localization of silver in zebrafish (*Danio rerio*).

- 547 Environ. Pollut. 206, 73-79.
- 548 Kim, D., Chae, Y. and An, Y.J. (2017) Mixture Toxicity of Nickel and Microplastics
549 with Different Functional Groups on *Daphnia magna*. Environ. Sci. Technol. 51(21),
550 12852-12858.
- 551 Koelmans, A.A., Bakir, A., Burton, G.A. and Janssen, C.R. (2016) Microplastic as a
552 Vector for Chemicals in the Aquatic Environment: Critical Review and
553 Model-Supported Reinterpretation of Empirical Studies. Environ. Sci. Technol. 50(7),
554 3315-3326.
- 555 Kołodzyńska, D., Wnętrzak, R. and Hubicki, Z. (2012) Kinetic and adsorptive
556 characterization of biochar in metal ions removal. Chem. Eng. J. 197, 295-305.
- 557 Koukina, S.E., Lobus, N.V., Peresyphkin, V.I., Dara, O.M. and Smurov, A.V. (2016)
558 Abundance, distribution and bioavailability of major and trace elements in surface
559 sediments from the Cai River estuary and Nha Trang Bay (South China Sea, Vietnam).
560 Estuarine, Coastal Shelf. Sci., 1-11.
- 561 Lares, M., Ncibi, M.C., Sillanpaa, M. and Sillanpaa, M. (2018) Occurrence,
562 identification and removal of microplastic particles and fibers in conventional
563 activated sludge process and advanced MBR technology. Water Res. 133, 236-246.
- 564 Leslie, H.A., Brandsma, S.H., van Velzen, M.J. and Vethaak, A.D. (2017)
565 Microplastics en route: Field measurements in the Dutch river delta and Amsterdam
566 canals, wastewater treatment plants, North Sea sediments and biota. Environ. Int. 101,
567 133-142.
- 568 Li, J., Zhang, K. and Zhang, H. (2018a) Adsorption of antibiotics on microplastics.
569 Environ. Pollut. 237, 460-467.
- 570 Li, S., Liu, H. and Zeng, F. (2018b) Aggregation kinetics of microplastics in aquatic
571 environment: Complex roles of electrolytes, pH, and natural organic matter. Environ.
572 Pollut. 237, 126-132.
- 573 Li, X., Chen, L., Mei, Q., Dai, X. and Zeng, E.Y. (2018c) Microplastics in sewage
574 sludge from the wastewater treatment plants in China. Water Res. 142, 75-85.
- 575 Li, X., Chen, L., Dai, X., Mei, Q. and Ding, G. (2017) Thermogravimetry–Fourier
576 transform infrared spectrometry–mass spectrometry technique to evaluate the effect of
577 anaerobic digestion on gaseous products of sewage sludge sequential pyrolysis. J.
578 Anal. Appl. Pyrol. 126, 288-297.
- 579 Li, X., Dai, X., Dai, L. and Liu, Z. (2015) Two-dimensional FTIR correlation
580 spectroscopy reveals chemical changes in dissolved organic matter during the
581 biodrying process of raw sludge and anaerobically digested sludge. RSC Adv. 5(100),
582 82087-82096.
- 583 Li, X., Dai, X., Takahashi, J. and Li, N. (2014) New insight into chemical changes of
584 dissolved organic matter during anaerobic digestion of dewatered sewage sludge
585 using EEM-PARAFAC and two-dimensional FTIR correlation spectroscopy.
586 Bioresour. Technol. 159, 412-420.
- 587 Lu, S., Zhu, K., Song, W. and Song, G. (2018) Impact of water chemistry on surface
588 charge and aggregation of polystyrene microspheres suspensions. Sci. Total. Environ.

- 589 630, 951-959.
- 590 Luis, L.G., Ferreira, P., Fonte, E., Oliveira, M. and Guilhermino, L. (2015) Does the
591 presence of microplastics influence the acute toxicity of chromium(VI) to early
592 juveniles of the common goby (*Pomatoschistus microps*)? A study with juveniles from
593 two wild estuarine populations. *Aquat. Toxicol.* 164, 163-174.
- 594 Mahon, A.M., O'Connell, B., Healy, M.G. and O'Connor, I. (2017) Microplastics in
595 Sewage Sludge: Effects of Treatment. *Environ. Sci. Technol.* 51(2), 810-818.
- 596 Mason, S.A., Garneau, D., Sutton, R., Chu, Y., Ehmann, K., Barnes, J., Fink, P.,
597 Papazissimos, D. and Rogers, D.L. (2016) Microplastic pollution is widely detected in
598 US municipal wastewater treatment plant effluent. *Environ. Pollut.* 218, 1045-1054.
- 599 Matsui, M., Kiyozumi, Y., Mizushima, Y., Sakaguchi, K. and Mizukami, F. (2015)
600 Adsorption and desorption behavior of basic proteins on zeolites. *Sep. Purif. Technol.*
601 149, 103-109.
- 602 Melo, D.Q. and Neto, V.O.S. (2013) Adsorption Equilibria of Cu^{2+} , Zn^{2+} , and Cd^{2+}
603 on EDTA-Functionalized Silica Spheres. *J. Chem. Eng. Data.* 58(3), 798-806.
- 604 Murphy, F., Ewins, C., Carbonnier, F. and Quinn, B. (2016) Wastewater Treatment
605 Works (WwTW) as a Source of Microplastics in the Aquatic Environment. *Environ.*
606 *Sci. Technol.* 50(11), 5800-5808.
- 607 Narancic, T., Verstichel, S. and Babu Padamati, R. (2018) Biodegradable Plastic
608 Blends Create New Possibilities for End-of-Life Management of Plastics but They
609 Are Not a Panacea for Plastic Pollution. *Environ. Sci. Technol.* 52(18), 10441-10452.
- 610 Nies, D.H. (1991) Microbial heavy-metal resistance *Appl. Microbiol. Biotechnol.* (51),
611 730-750.
- 612 Nizzetto, L., Futter, M. and Langaas, S. (2016) Are Agricultural Soils Dumps for
613 Microplastics of Urban Origin? *Environ. Sci. Technol.* 50(20), 10777-10779.
- 614 Noda, I., Ozaki, Y. (2005) Two-Dimensional Correlation Spectroscopy: Applications
615 in Vibrational and Optical Spectroscopy. Wiley.com.
- 616 O'Connor, I.A., Golsteijn, L. and Hendriks, A.J. (2016) Review of the partitioning of
617 chemicals into different plastics: Consequences for the risk assessment of marine
618 plastic debris. *Mar. Pollut. Bull.* 113(1-2), 17-24.
- 619 Pascall, M.A., Zabik, M.E., Zabik, M.J. and Hernandez, R.J. (2005) Uptake of
620 polychlorinated biphenyls (PCBs) from an aqueous medium by polyethylene,
621 polyvinyl chloride, and polystyrene films. *J. Agri. Food Chem.* 53(1), 164-169.
- 622 Restrepo-Flórez, J.-M., Bassi, A. and Thompson, M.R. (2014) Microbial degradation
623 and deterioration of polyethylene – A review. *Int. Biodeterior. Biodegrad.* 88, 83-90.
- 624 Rocha, C.G., Zaia, D.A., Alfaya, R.V. and Alfaya, A.A. (2009) Use of rice straw as
625 biosorbent for removal of Cu(II) , Zn(II) , Cd(II) and Hg(II) ions in industrial effluents.
626 *J. Hazard. Mater.* 166(1), 383-388.
- 627 Sebillé, E.v. (2015) A global inventory of small floating plastic debris. *Environ. Res.*
628 *Lett.* 10, 124006.
- 629 Shah, A.A., Hasan, F., Hameed, A. and Ahmed, S. (2008) Biological degradation of
630 plastics: A comprehensive review. *Biotechnol. Adv.* 26(3), 246-265.

- 631 Sheng, G.P., Yu, H.Q. and Li, X.Y. (2010) Extracellular polymeric substances (EPS)
632 of microbial aggregates in biological wastewater treatment systems: a review.
633 *Biotechnol. Adv.* 28(6), 882-894.
- 634 Smith, S.R. (2009) A critical review of the bioavailability and impacts of heavy metals
635 in municipal solid waste composts compared to sewage sludge. *Environ. Int.* 35(1),
636 142-156.
- 637 Song, Y.K., Hong, S.H., Jang, M. and Shim, W.J. (2017) Combined Effects of UV
638 Exposure Duration and Mechanical Abrasion on Microplastic Fragmentation by
639 Polymer Type. *Environ. Sci. Technol.* 51(8), 4368-4376.
- 640 Talvitie, J., Mikola, A., Koistinen, A. and Setälä, O. (2017) Solutions to microplastic
641 pollution - Removal of microplastics from wastewater effluent with advanced
642 wastewater treatment technologies. *Water Res.* 123, 401-407.
- 643 Ter Halle, A., Ladirat, L., Gendre, X., Goudouneche, D., Pusineri, C., Routaboul, C.,
644 Tenailleau, C., Duployer, B. and Perez, E. (2016) Understanding the Fragmentation
645 Pattern of Marine Plastic Debris. *Environ. Sci. Technol.* 50(11), 5668-5675.
- 646 Teuten, E.L., Saquing, J.M., Knappe, D.R.U. and Barlaz, M.A. (2009) Transport and
647 release of chemicals from plastics to the environment and to wildlife. *Philos. Trans. R.*
648 *Soc. B.* 364(1526), 2027-2045.
- 649 Turner, A. and Holmes, L.A. (2015) Adsorption of trace metals by microplastic pellets
650 in fresh water. *Environ. Chem.* 12(5), 600-610.
- 651 Vimala, R. and Das, N. (2009) Biosorption of cadmium (II) and lead (II) from
652 aqueous solutions using mushrooms: a comparative study. *J. Hazard. Mater.* 168(1),
653 376-382.
- 654 Wang, F., Shih, K.M. and Li, X.Y. (2015) The partition behavior of
655 perfluorooctanesulfonate (PFOS) and perfluorooctanesulfonamide (FOSA) on
656 microplastics. *Chemosphere* 119, 841-847.
- 657 Wang, F., Wong, C.S. and Zeng, E.Y. (2018) Interaction of toxic chemicals with
658 microplastics: A critical review. *Water Res.* 139, 208-219.
- 659 Wang, J., Peng, J., Tan, Z. and Gao, Y. (2017) Microplastics in the surface sediments
660 from the Beijiing River littoral zone: Composition, abundance, surface textures and
661 interaction with heavy metals. *Chemosphere* 171, 248-258.
- 662 Wang, W. and Wang, J. (2018) Comparative evaluation of sorption kinetics and
663 isotherms of pyrene onto microplastics. *Chemosphere* 193, 567-573.
- 664 Wei, D., Li, M., Wang, X., Han, F., Li, L., Guo, J., Ai, L., Fang, L., Liu, L., Du, B. and
665 Wei, Q. (2016) Extracellular polymeric substances for Zn (II) binding during its
666 sorption process onto aerobic granular sludge. *J. Hazard. Mater.* 301, 407-415.
- 667 Wei, H., Gao, B., Ren, J., Li, A. and Yang, H. (2018) Coagulation/flocculation in
668 dewatering of sludge: A review. *Water Res.* 143, 608-631.
- 669 Wijesekara, H., Bolan, N.S. and Bradney, L. (2018) Trace element dynamics of
670 biosolids-derived microbeads. *Chemosphere* 199, 331-339.
- 671 Wu, C.C., Bao, L.J., Liu, L.Y., Shi, L., Tao, S. and Zeng, E.Y. (2017) Impact of
672 Polymer Colonization on the Fate of Organic Contaminants in Sediment. *Environ. Sci.*

- 673 Technol. 51(18), 10555-10561.
- 674 Xu, B. and Liu, F. (2018) Microplastics play a minor role in tetracycline sorption in
675 the presence of dissolved organic matter. Environ. Pollut. 240, 87-94.
- 676 Xu, Q., Li, X., Ding, R., Wang, D., Liu, Y., Wang, Q., Zhao, J., Chen, F., Zeng, G.,
677 Yang, Q. and Li, H. (2017) Understanding and mitigating the toxicity of cadmium to
678 the anaerobic fermentation of waste activated sludge. Water Res. 124, 269-279.
- 679 Yang, Y. and Chun, Y. (2004) pH-Dependence of Pesticide Adsorption by
680 Wheat-Residue-Derived Black Carbon. Langmuir 20, 6736-6741.
- 681 Yoshida, S. (2016) A bacterium that degrades and assimilates poly(ethylene
682 terephthalate). Science 351(6278), 1196-1199.
- 683 Zhao, Y. (2015) Investigation on the properties of sewage sludge of WWTPs in China
684 and Experiments on sand removal of sludge, Tongji University, Shanghai. (In
685 Chinese)
- 686 Zubris, K.A. and Richards, B.K. (2005) Synthetic fibers as an indicator of land
687 application of sludge. Environ. Pollut. 138(2), 201-211.
- 688

689 Table 1. Properties of sewage sludge samples derived from three wastewater treatment
 690 plants (WWTPs).

Parameters	Sludge samples			
	S1	S2	S3	
pH	7.29	6.88	7.38	
TS (%)	15.42 ± 0.1	15.42 ± 0.1	16.60 ± 0.5	
VS/TS (%)	58.66 ± 0.2	64.15 ± 0.3	59.61 ± 0.2	
Elemental composition (%)	C	32.13 ± 0.16	32.89 ± 0.63	33.84 ± 0.28
	H	5.53 ± 0.0265	5.90 ± 0.29	5.15 ± 0.14
	N	4.78 ± 0.025	4.45 ± 0.08	6.02 ± 0.08
	S	0.94 ± 0.007	1.14 ± 0.15	0.85 ± 0.02
Abundance of MPs (particles kg ⁻¹ dry sludge)	13787	15080	37463	

691 Table 2. Constants defining Cd adsorption on the virgin and sludge-based MPs
 692 according to the isotherm models.

MPs	Langmuir	Freundlich	Dubbin-Radushkevich
PE	$k_L=0.414 \text{ L } \mu\text{g}^{-1}$ $q_{\max}=234.5 \mu\text{g g}^{-1}$ $R^2=0.92$ $p=0.000$	$k_F=4.53 \mu\text{g}^{1-1/n} \text{ g}^{-1} \text{ L}^{1/n}$ $n=3.7$ $R^2=0.89$ $p=0.001$	$q_{DR}=202.6 \mu\text{g g}^{-1}$ $R^2=0.79$ $p=0.006$
PA	$k_L=0.320 \text{ L } \mu\text{g}^{-1}$ $q_{\max}=339.6 \mu\text{g g}^{-1}$ $R^2=0.89$ $p=0.005$	$k_F=5.28 \mu\text{g}^{1-1/n} \text{ g}^{-1} \text{ L}^{1/n}$ $n=2.58$ $R^2=0.83$ $p=0.011$	$q_{DR}=214.4 \mu\text{g g}^{-1}$ $R^2=0.56$ $p=0.006$
PP	$k_L=0.675 \text{ L } \mu\text{g}^{-1}$ $q_{\max}=199.2 \mu\text{g g}^{-1}$ $R^2=0.91$ $p=0.003$	$k_F=4.71 \mu\text{g}^{1-1/n} \text{ g}^{-1} \text{ L}^{1/n}$ $n=3.67$ $R^2=0.67$ $p=0.047$	$q_{DR}=201.5 \mu\text{g g}^{-1}$ $R^2=0.84$ $p=0.029$
PS	$k_L=0.516 \text{ L } \mu\text{g}^{-1}$ $q_{\max}=69.9 \mu\text{g g}^{-1}$ $R^2=0.81$ $p=0.037$	$k_F=1.11 \mu\text{g}^{1-1/n} \text{ g}^{-1} \text{ L}^{1/n}$ $n=2.23$ $R^2=0.662$ $p=0.094$	$q_{DR}=103.7 \mu\text{g g}^{-1}$ $R^2=0.83$ $p=0.029$
PVC	$k_L=0.845 \text{ L } \mu\text{g}^{-1}$ $q_{\max}=222.2 \mu\text{g g}^{-1}$ $R^2=0.64$ $p=0.012$	$k_F=0.813 \mu\text{g}^{1-1/n} \text{ g}^{-1} \text{ L}^{1/n}$ $n=1.24$ $R^2=0.94$ $p=0.007$	$q_{DR}=67.6 \mu\text{g g}^{-1}$ $R^2=0.03$ $p=0.784$
Sludge-based MPs	$k_L=0.547 \text{ L } \mu\text{g}^{-1}$ $q_{\max}=2.52 \text{ mg g}^{-1}$ $R^2=0.98$ $p=0.000$	$k_F=50.6 \mu\text{g}^{1-1/n} \text{ g}^{-1} \text{ L}^{1/n}$ $n=4.67$ $R^2=0.91$ $p=0.000$	$q_{DR}=1.67 \text{ mg g}^{-1}$ $R^2=0.70$ $p=0.784$

693 Figure Captions

694 Figure 1. The content of metals in sewage sludge and adsorbed on the sludge-based

695 MPs (A-C) and virgin MPs (D) (mean value \pm SD, n=3).

696 Figure 2. Sorption isotherms of Cd on the virgin and sludge-based MPs. (mean value \pm

697 SD, n=3).

698 Figure 3. SEM graphs of the virgin and sludge-based MPs (V, virgin MPs; S,

699 sludge-based MPs).

700 Figure 4. Synchronous (left) and asynchronous (right) 2D correlation maps generated

701 from 900–1300 cm^{-1} (above) and 1350–1600 cm^{-1} (below) regions of FTIR

702 spectra of the sludge-based MPs adsorbing increasing contents of Cd.

703 Figure 5. The influence of pH value, silica sand (SS), protein, and humic substances on

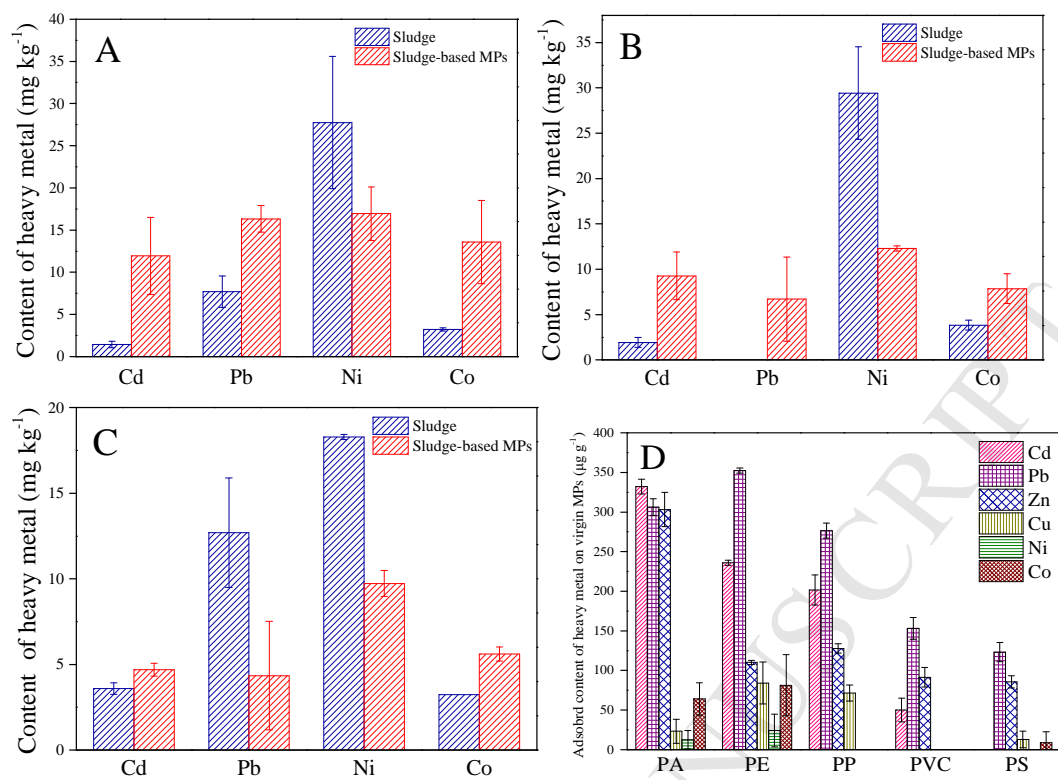
704 adsorption of Cd on the MPs (mean value \pm SD, n=3).

705 Figure 6. Principal component analysis (PCA) of different types of MPs according to

706 their maximum Cd adsorption amount and changing characteristics of

707 adsorbed Cd content under the influence of pH, and sludge IOM and OM

708 components.

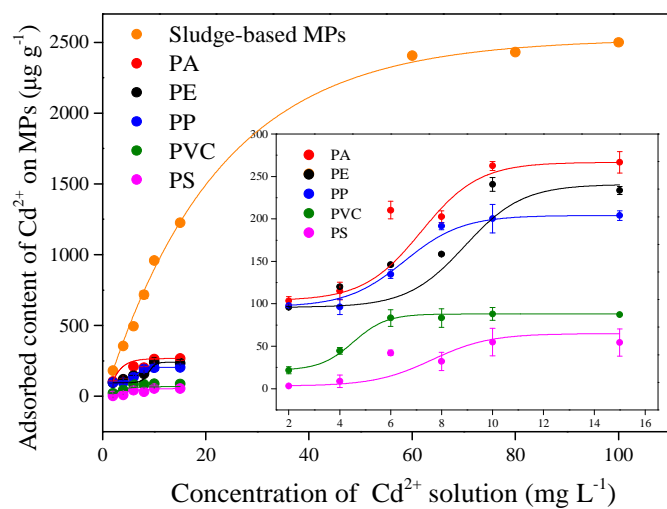


709

710

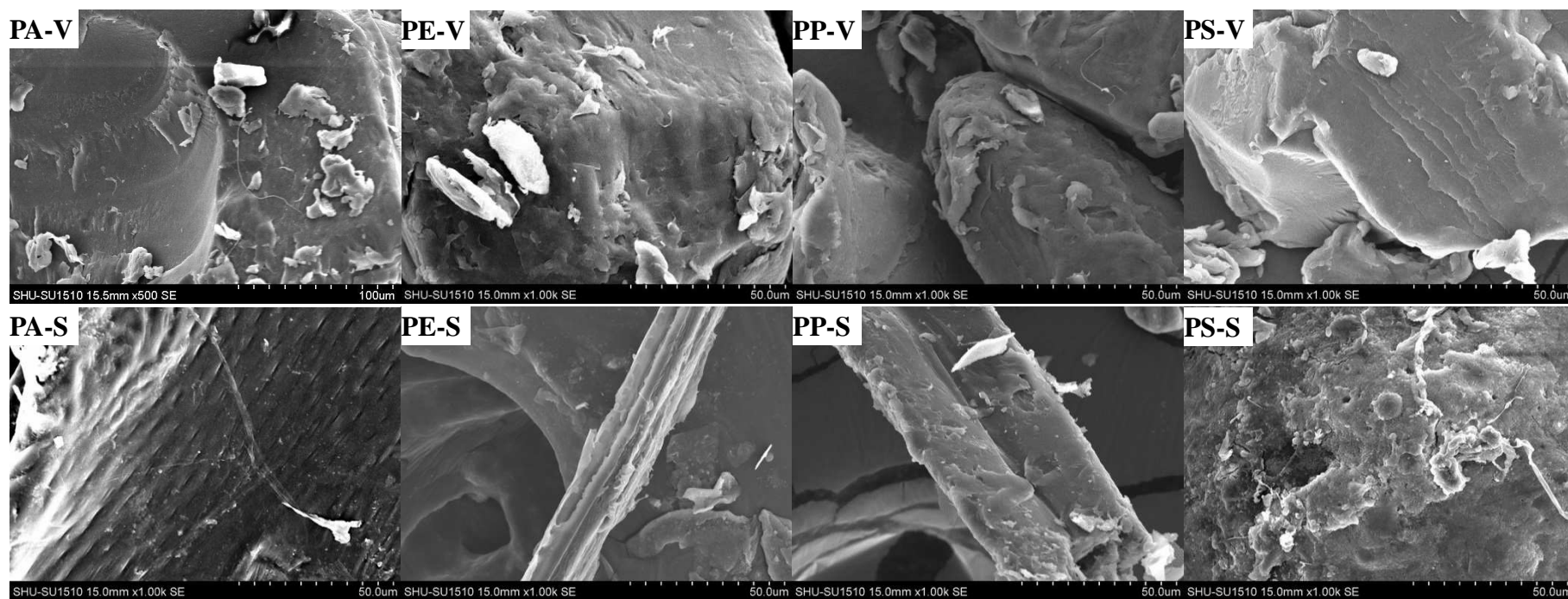
711

Figure 1.



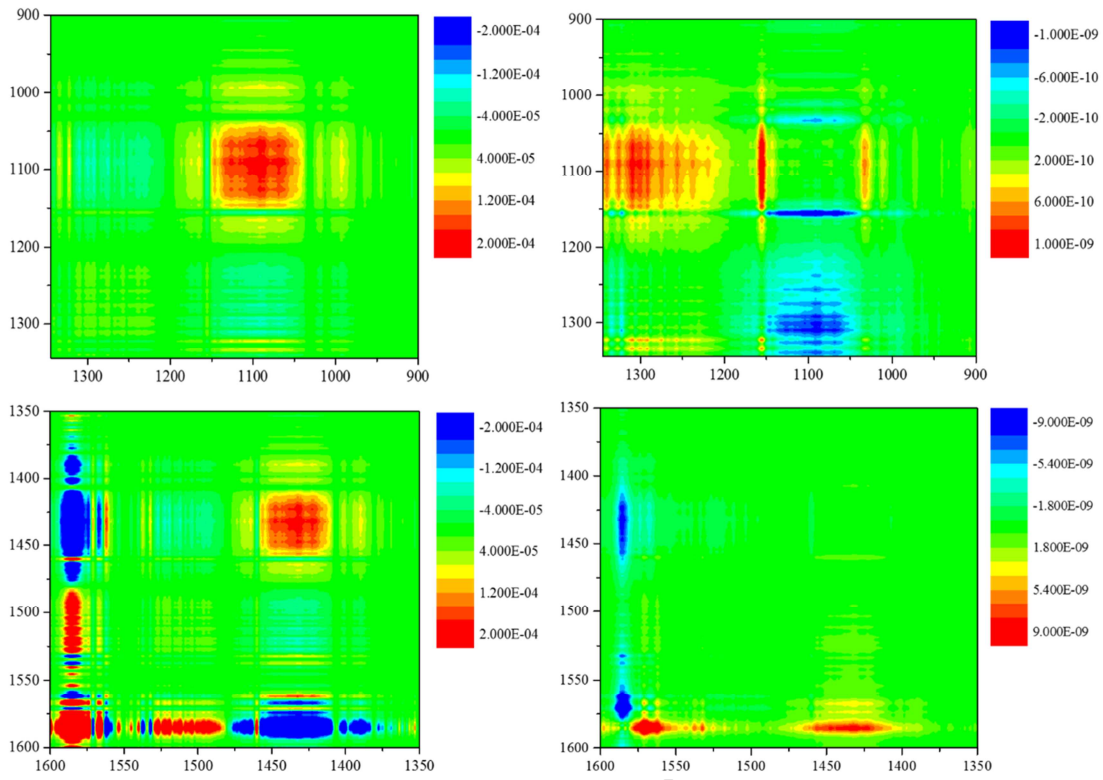
712

713 Figure 2.



714
715

Figure 3.

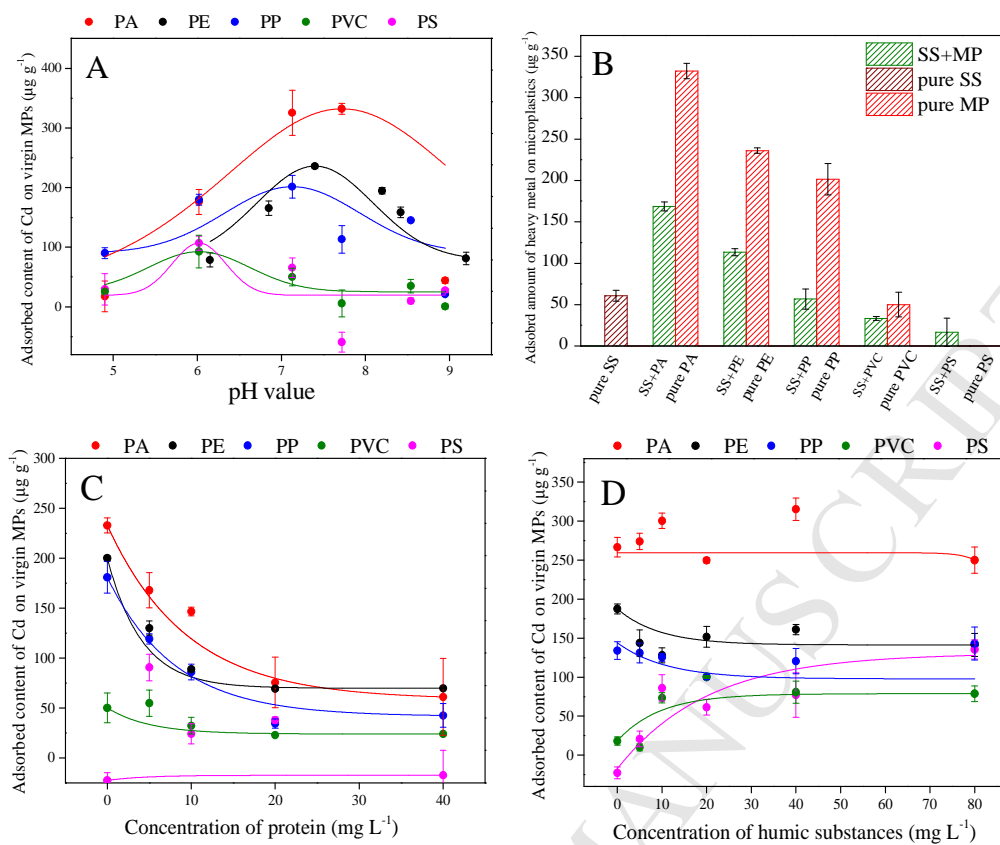


716

717

Figure 4.

718



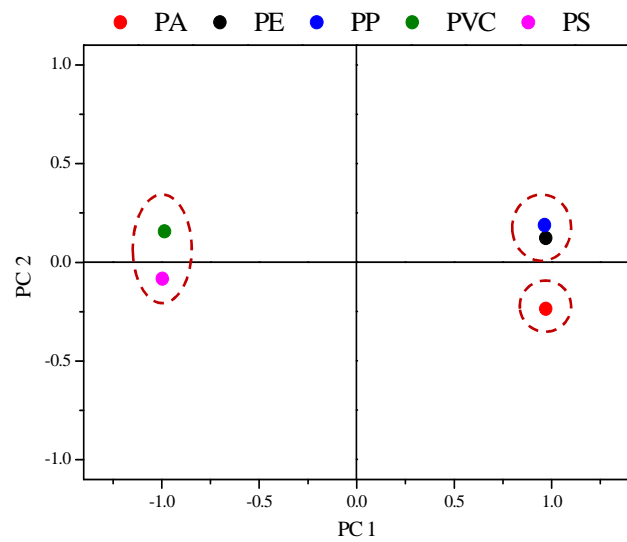
719

720

721

722

Figure 5.



723

724 Figure 6.

725

Highlights

- Some metal pollutants such as Cd and Ni are accumulated on sludge-based MPs
- The contents of metal iron adsorbed on sludge-based and virgin MPs were compared
- An increase in adsorption potential of sludge-based MPs after wastewater treatment
- The enhancement of MPs is resulted from changes in their physicochemical properties
- Types of plastics, pH and sludge components affect the adsorption of MPs to Cd

Conflict of interest

We declare that we do not have any commercial or associative interest that represents a conflict of interest in connection with the work submitted.

ACCEPTED MANUSCRIPT